Missouri University of Science and Technology
Scholars' Mine

Physics Faculty Research & Creative Works | Physics

01 Feb 2013

Imaging the Anisotropic Nonlinear Meissner Effect in Nodal YBa $_2Cu_3O_{7-\delta}$ Thin-Film Superconductors

Alexander P. Zhuravel

Behnood G. Ghamsari

Cihan Kurter
Missouri University of Science and Technology, kurterc@mst.edu

Philipp Jung

et. al. For a complete list of authors, see https://scholarsmine.mst.edu/phys_facwork/1455

Follow this and additional works at: https://scholarsmine.mst.edu/phys_facwork

 Part of the Physics Commons

Recommended Citation

A. P. Zhuravel et al., "Imaging the Anisotropic Nonlinear Meissner Effect in Nodal YBa $_2Cu_3O_{7-\delta}$ Thin-Film Superconductors," *Physical Review Letters*, vol. 110, no. 8, pp. 087002-1-087002-5, American Physical Society (APS), Feb 2013.
The definitive version is available at https://doi.org/10.1103/PhysRevLett.110.087002

This Article - Journal is brought to you for free and open access by Scholars' Mine. It has been accepted for inclusion in Physics Faculty Research & Creative Works by an authorized administrator of Scholars' Mine. This work is protected by U. S. Copyright Law. Unauthorized use including reproduction for redistribution requires the permission of the copyright holder. For more information, please contact scholarsmine@mst.edu.

Imaging the Anisotropic Nonlinear Meissner Effect in Nodal $YBa_2Cu_3O_{7-\delta}$ Thin-Film Superconductors

Alexander P. Zhuravel,[1] B. G. Ghamsari,[2] C. Kurter,[2] P. Jung,[3] S. Remillard,[4] J. Abrahams,[2] A. V. Lukashenko,[3] Alexey V. Ustinov,[3] and Steven M. Anlage[2,3]

[1]*B. Verkin Institute for Low Temperature Physics and Engineering, National Academy of Sciences of Ukraine, UA-61103 Kharkov, Ukraine*

[2]*CNAM, Physics Department, University of Maryland, College Park, Maryland 20742-4111, USA*

[3]*Physikalisches Institut and DFG-Center for Functional Nanostructures (CFN), Karlsruhe Institute of Technology, DE-76128 Karlsruhe, Germany*

[4]*Physics Department, Hope College, 27 Graves Place, Holland, Michigan 49422, USA*

(Received 1 August 2012; published 21 February 2013)

We have directly imaged the anisotropic nonlinear Meissner effect in an unconventional superconductor through the nonlinear electrodynamic response of both (bulk) gap nodes and (surface) Andreev bound states. A superconducting thin film is patterned into a compact self-resonant spiral structure, excited near resonance in the radio-frequency range, and scanned with a focused laser beam perturbation. At low temperatures, direction-dependent nonlinearities in the reactive and resistive properties of the resonator create photoresponse that maps out the directions of nodes, or of bound states associated with these nodes, on the Fermi surface of the superconductor. The method is demonstrated on the nodal superconductor $YBa_2Cu_3O_{7-\delta}$ and the results are consistent with theoretical predictions for the bulk and surface contributions.

DOI: 10.1103/PhysRevLett.110.087002 PACS numbers: 74.25.N−, 74.20.Rp, 74.45.+c, 74.72.Gh

Introduction.—The Meissner effect is the spontaneous exclusion of magnetic flux from the bulk of a superconductor and is one of the hallmarks of superconductivity. In the presence of a magnetic field, a superconductor must invest kinetic energy in a supercurrent flow to screen out the applied field. This reduces the free energy difference between the superconducting and normal states, resulting in a reduction in magnitude of the superconducting order parameter. This in turn leads to a field- and current-dependent magnetic penetration depth, diamagnetic moment, etc., and is referred to as the nonlinear Meissner effect (NLME). Microscopically, the NLME arises when Cooper pairs at the leading edge of the current-carrying Fermi surface can undergo depairing into available quasiparticle states at the back end and create a quasiparticle backflow current [1]. Conventional (fully gapped) superconductors show the strongest nonlinearities near T_c, and have exponentially suppressed nonlinear response at low temperatures, $T \ll T_c$. Unconventional superconductors with nodes in the superconducting energy gap are expected to have a strong nonlinear Meissner effect at low temperatures, due to the nodal excitations out of the superconducting ground state [2]. In addition, this nonlinear response should be anisotropic, reflecting the locations of nodes of the gap on the Fermi surface.

For a d_{x2-y2} gap on a circular cut of the cylindrical Fermi surface, typical of cuprate superconductors, theoretical treatments of the anisotropic NLME (aNLME) predicted a $1/\sqrt{2}$ anisotropy at zero temperature [2,3]. Later, the theory was reformulated in terms of nonlinear microwave intermodulation response of a nodal superconductor [4–6], and the temperature dependence of the NLME and its anisotropy was worked out. The dependence of the superfluid density n_s on supercurrent density $\vec{J}_s$, for sufficiently small currents, is given by $n_s(T, \vec{J}_s) = n_s(T) \times [1 - b_\Theta(T)(J_s/J_c)^2]$, where J_c is the critical current density, and $b_\Theta(T)$ is the nonlinearity coefficient dependent on the direction (angle Θ) of $\vec{J}_s$ [4]. It was found that the anisotropy in the NLME of cuprates is weak at high temperatures, and only becomes significant for $T/T_c < 0.6$ [5]. In addition, it was found that $b_\Theta(T)$ is expected to grow as $1/T$ for $T/T_c < 0.2$ [4], before crossing over to another temperature dependence, depending on the purity of the material [3,6,7].

Early experiments to detect the aNLME of cuprates through transverse magnetization [8,9], magnetic penetration depth [10–12], and surface impedance [13] measurements did not establish conclusive evidence of the effect [7]. Later, sensitive nonlinear microwave measurement techniques established the existence of the NLME in cuprates from the temperature dependence of the intermodulation power at low temperatures [14–16], although the anisotropy of the effect was not measured. Although other thermodynamic measurements have shown evidence of an anisotropic energy gap in various superconductors [17–19], there are no unambiguous measurements of the aNLME in cuprates, to our knowledge [20]. In contrast to quasiparticle transport methods [17–19], the present method utilizes the bulk superfluid response to identify the nodal directions [21].

 © 2013 American Physical Society

An additional contribution to the NLME in unconventional superconductors arises from Andreev bound states (ABS) [22], created, for example, on the {110} surfaces of a d_{x2-y2} superconductor. These states give rise to a *paramagnetic* contribution to the screening [23]. For cuprates, {110} interfaces occur at twin boundaries, which are formed spontaneously during epitaxial film growth. The NLME associated with ABS has been established by tunneling [24], and penetration depth measurements [25,26], for example. Theory by Barash, Kalenkov, and Kurkijärvi (BKK) [27] and Zare, Dahm, and Schopohl (ZDS) [28] predicts an aNLME associated with ABS having a strong temperature dependence at low temperatures, eventually dominating that due to nodal excitations.

Here we establish a new method to both quantitatively measure and image the aNLME from nodes in the superconducting gap using a novel rf resonant technique combined with laser scanning microscopy.

Experiment.—We employ a self-resonant superconducting structure based on a thin film Archimedean spiral geometry. The spiral has an inner diameter of 4.4 mm, an outer diameter of 6 mm, and consists of 40 turns of nominally 10 μm width thin film stripe with 10 μm spacing, winding continuously from the inner to outer radii with Archimedean form [see the schematic in Fig. 1(a)]. The structure has considerable inductance and capacitance, making it a compact self-resonant meta-atom for use in superconducting metamaterials [29,30]. When made from superconducting materials such as Nb and $YBa_2Cu_3O_{7-\delta}$ (YBCO), the spiral has a fundamental resonance in the vicinity of 75 MHz, and many overtones extending above 1 GHz. The distribution of standing wave currents on the spiral in the first few modes are well approximated as those of a resonant vibrating string held fixed at both ends, and then wrapped into a spiral, as verified by detailed laser scanning microscope (LSM) imaging [31–33] (also, see the Supplemental Material [34]). A unique property of the resonant spiral is the fact that the currents in the low-order modes circle the spiral many times, repeatedly sampling all parts of the in-plane Fermi surface [33].

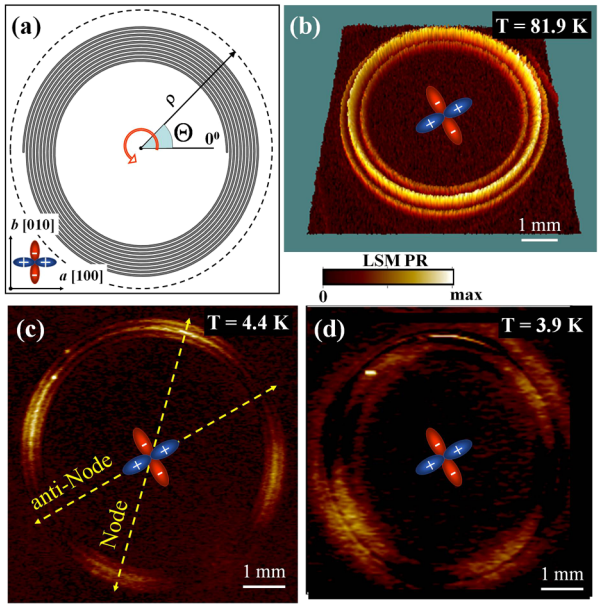

FIG. 1 (color online). (a) Schematic diagram of spiral geometry, definition of radial (ρ) and angular (Θ) coordinates, and directions of the crystallographic a and b directions, along with the orientation of the d-wave gap in YBCO. (b)–(d) LSM photoresponse images of a YBCO/LAO spiral resonator in the third harmonic mode at temperatures of (b) 81.9, (c) 4.40, and (d) 3.90 K. Also shown is the d-wave gap orientation as determined from twin domain boundary directions in the substrate.

The epitaxial and in-plane oriented YBCO films on $LaAlO_3$ (LAO) were deposited by *in situ* off-axis magnetron sputtering to a thickness of 300 nm [35]. Similar YBCO films on CeO_2 buffered sapphire and on MgO were deposited by thermal coevaporation to a thickness of 300 and 700 nm, respectively [36]. The 200 nm thick Nb films were deposited on quartz substrates at room temperature by rf sputtering [29,31]. All films were patterned into spiral resonators by contact photolithography and either wet or dry chemical etching.

The LSM operates by scanning a focused laser spot (wavelength 640 nm) over the surface of the spiral while it is excited near its rf resonance with excitation and pickup loops above and below the plane of the film (see the Supplemental Material [34]). Details of the rf and laser excitations of the spirals have been previously published [29,31–33]. The spiral develops a photoresponse due to pair breaking and localized heating, producing a change in its resonant frequency and quality factor [37,38]. The laser intensity is modulated at 100 kHz, and the changes in rf transmission at a fixed frequency are phase sensitively detected, resulting in a photoresponse (PR) signal consisting of both a magnitude and phase. The peak laser intensity can be varied between 150 μW and 1.6 mW. The laser spot (about 20 μm diameter) is scanned over the sample to create a two-dimensional PR image. To first approximation, the PR magnitude can be interpreted as the distribution of rf currents $J_{\rm rf}^2(\rho, \Theta)$ [32,33,37–40] (also, see the Supplemental Material [34]).

The aNLME is expected to create the following PR contrast [4,41]. For a d_{x2-y2} gap on a circular Fermi surface one expects PR $\sim 1 + \sin^2(2\Theta)$ with $\Theta = 0$ along the Cu-O-Cu bond direction of YBCO [see Fig. 1(a)]. In addition, the PR amplitude should vary as $1/T^2$ for $T/T_c < 0.2$ and $J_{\rm rf}/J_c < T/T_c$, where $J_{\rm rf}$ is the rf current density induced in the sample. It is also expected that the LSM PR is proportional to rf power and proportional to the intensity of the laser light. As deduced from BKK and ZDS, the contribution to LSM PR from ABS should be centered on {110} surfaces of the material, have a stronger temperature dependent PR $\sim 1/T^4$, have the opposite sign of PR from the nodal aNLME (due to the paramagnetic nature of the ABS), and be a linear function of rf and laser power up to rf fields on the order of a few mT [27,28].

Results.—Figure 1 shows LSM PR images of a single YBCO/LAO spiral in a resonant mode at three different temperatures, 81.9, 4.4, and 3.9 K. The image is of the third harmonic mode and shows three nearly circular distinct bands of enhanced PR, corresponding to the three half-wavelengths of current distributed over the 40 turns of superconducting wire [31–33] (also, see the Supplemental Material [34]). One notes that the PR is isotropic in its angular distribution around the spiral at 81.9 K [Fig. 1(b)]. However, the LSM PR image of the same mode at 4.40 K [Fig. 1(c)] shows four distinct enhancements of PR at regular angular intervals around the spiral. As the sample is cooled further (below about 4.30 K for this particular sample), a new set of enhanced-PR features are observed in Fig. 1(d), but now rotated 45° relative to those at 4.40 K. Images of Nb spirals of nominally identical geometry in the same mode do not show this anisotropic PR at any temperature below the transition temperature. The above anisotropy and rotation behavior is observed to hold for the YBCO/LAO spiral excited into all modes, from the fundamental through the 8th mode (the highest examined).

Figure 2 shows the radially (ρ)-integrated PR as a function of angle for a YBCO/LAO thin film spiral resonator taken at a temperature of 4.66 K in the 7th mode at 450.22 MHz, shown in the inset. The zero-angle (Cu-O-Cu bond) direction was determined from the visible twinning structure of the LAO substrate. Utilizing the fact that the YBCO film was grown *epitaxially* and in-plane oriented on LAO, the observation that the PR maxima are aligned along the linear twin domain structures in the substrate, and the fact that the twin boundaries are aligned at 45° to the Cu-O-Cu bond direction [42], we deduced that the $\Theta = 0$ direction is at 45° to the twin domain structure of the substrate. Figure 2 shows a fit of the data to $\mathrm{PR}(\Theta) = 1 + A\sin^2(2\Theta)$, resulting in a fit value $A = 1.05 \pm 0.02$, close to the value of 1 expected for a simple d_{x2-y2} gap on a circular Fermi surface.

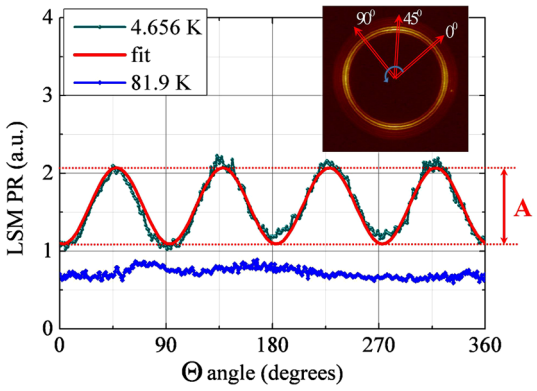

FIG. 2 (color online). Plot of radially integrated and unwrapped photoresponse (PR) vs angle on the YBCO/LAO spiral at 81.9 and 4.66 K, along with a fit of the low-temperature integrated $\mathrm{PR}(\Theta)$ to the simple d-wave angular dependence. Inset shows PR image of $YBCO/LaAlO_3$ thin film spiral resonator taken at a temperature of 4.656 K in the 7th mode at 450.22 MHz.

The PR images in the "rotated" state at lower temperatures [Fig. 1(d)] also show fourfold character, but are relatively diffuse in appearance, and display dramatically stronger PR as the temperature is lowered. To understand these properties, we examine the temperature dependence and phase of the photoresponse along the nodal ($\Theta = \pi/4$) and antinodal ($\Theta = 0$) directions of the superconducting gap. Figure 3 shows a plot of PR magnitude vs temperature for nodal and antinodal regions of a YBCO/sapphire spiral resonator. In the nodal direction the PR is of significant magnitude at a temperature of 6.6 K, but decreases in magnitude as temperature is lowered. The PR goes to near-zero levels and changes phase by π radians at a point that we call the "crossover temperature" [34]. Below this temperature the nodal PR magnitude increases dramatically. In the antinodal directions the PR is found to be smaller than the nodal PR at 6.6 K, but increases monotonically in magnitude with decreasing temperature, and has the same phase as the nodal PR below the crossover temperature.

A fit of the PR to the expected temperature dependence of nodal PR [temperature derivative of Eq. (16) of Ref. [28]], namely $\mathrm{PR} = A/T^2 - B/T^4 + \mathrm{const}$ (the first term is due to nodal NLME and the second due to ABS NLME) [28], is shown in the graphical inset of Fig. 3 for a YBCO/sapphire sample. The data are consistent with the predicted temperature dependence around the crossover temperature.

In all of these experiments we have verified that the LSM PR in the nodal direction is proportional to both rf

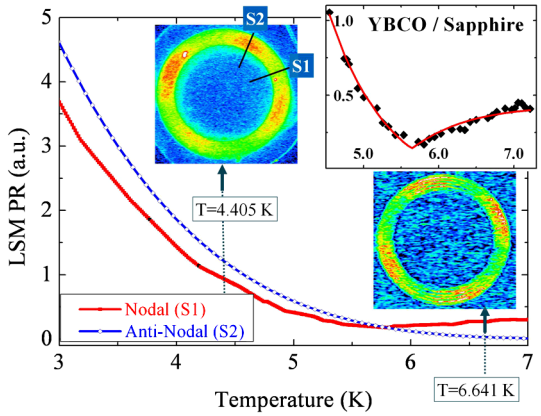

FIG. 3 (color online). Plot of temperature dependence of photoresponse (PR) magnitude taken at nodal and antinodal locations in a YBCO/sapphire spiral resonator. The antinodal PR has opposite sign to the nodal PR above the crossover temperature (5.63 K, as deduced from the fit). Graphical inset shows temperature dependence of the nodal PR magnitude near its crossover temperature, along with a fit to the form predicted by ZDS. Other insets show LSM PR magnitude images of YBCO/sapphire below (4.405 K) and above (6.641 K) its crossover temperature at 546.555 MHz. The phase of the PR in these images differ by π, corresponding to a sign reversal of the response.

power and to laser intensity. The LSM PR in the antinodal direction is linear at low laser powers, but becomes strongly nonlinear at higher laser powers. YBCO films grown on other substrates (MgO and sapphire) show the same general behavior described above as the samples on LAO. The spiral PR image insets of Fig. 3 show the YBCO/sapphire sample below (4.405 K) and above (6.641 K) the crossover temperature for this sample. We find that the PR maxima are aligned along the nodal directions of YBCO at higher temperatures, and then show a ''rotation'' by 45° at lower temperatures [43], although the crossover temperature is sample dependent (approximately 4–5 K for YBCO/LAO and 5–7 K for YBCO/MgO and YBCO/sapphire). This sample dependence may be associated with different abundances of exposed {110} facets, and twinning in each sample. YBCO films typically show twin separations less than 100 nm [44] and have complex bidirectional twinning, [45] meaning that our focused laser spot averages over a great many twin domains and any anisotropic effects of twinning will not be manifested on the scale of the spiral images. Note that the global nodal and antinodal directions are preserved in twinned structures.

Discussion.—A reorientation of specific heat oscillations with magnetic field direction (qualitatively similar to the crossover observed here) has been reported in superconductors with anisotropic order parameters [46,47]. However, specific heat measures the low-energy quasiparticle density of states [48] while our measurements probe the superfluid response and involve no dc magnetic field or vortices. Therefore, we do not believe that quasiparticle transport phenomena are the origin of the crossover observed in this Letter. On the other hand, the observed sign difference of LSM PR between the nodal and antinodal directions above the crossover temperature is consistent with the ZDS prediction for the NLME due to ABS [28]. The strong and monotonic temperature dependence of PR observed along the {110} directions of the film are also consistent with the ZDS prediction. The observed crossover temperature (4 to 7 K) is on the order of that predicted by ZDS, namely $T_c/\kappa^{1/2} \sim 10$ K, where κ is the Ginzburg-Landau parameter. Together, these results confirm the basic predictions of BKK and ZDS for the relative contributions of the nodal and ABS contributions to the NLME. Note that the use of thin film superconducting spiral resonators that expose many different crystallographic directions, and which have a large surface-to-volume ratio and high twin density, accentuates the contribution of ABS to the photoresponse.

In order to verify the above interpretation of the data, a number of potential artifacts and other interpretations of the PR images have been systematically explored. First is the possibility of anisotropic PR being created by the irregularly shaped excitation and rf pickup loops. The anisotropic PR did not change when the excitation loop was rotated relative to the sample. In addition, the anisotropic PR pattern rotated when the sample was rotated relative to the loops. We do not observe a significant degree of PR anisotropy in Nb spirals measured under similar conditions.

A second concern is that the PR temperature dependence arises from a growing thermal boundary resistance, $R_{\mathrm{bdy}} \sim 1/T^3$, between the thin film superconductor and the dielectric substrate [49]. However the strong temperature dependence is not observed in Nb/quartz samples, eliminating most of the cryostat components from generating this response. All YBCO samples (on LAO, MgO, and sapphire) show the strong PR temperature dependence at low temperatures. Nevertheless, we do believe that a thermal blockade may set in for the YBCO/LAO samples at low temperatures (< 3 K), resulting in diffuse PR images. This interpretation was independently verified through measurements of the PR thermal relaxation time as a function of temperature.

A third concern is that the twinned structure of the LAO substrate traps heat and channels it in specific directions, giving rise to the observed anisotropy. However, we observe the same anisotropy on YBCO/MgO and YBCO/sapphire films that do not have twinned substrates. The apparent rotation of the PR by 45° in a narrow temperature range in all of the YBCO samples also argues against a substrate-induced anisotropy. Next is the concern that the shape of the substrate dictates the anisotropy of the PR in the spiral. Numerical simulations of localized heating of a spiral on a square substrate under conditions similar to those of our YBCO samples showed a temperature anisotropy of only 1 part in 1000 imposed by the shape of the substrate, whereas the observed anisotropy is on the order of 50%. Finally is the concern that defects in the lithographic pattern of the spiral (namely, shorts between wires or opens) will create the anisotropic PR. We find that all YBCO spirals, from those with near-perfect lithography to those with defective patterns, all show the anisotropy and temperature dependent properties described above.

Conclusions.—We have measured and imaged the anisotropic nonlinear Meissner effect in an unconventional superconductor arising from both bulk and surface mechanisms. Our results are in detailed agreement with aNLME theoretical predictions based on both nodal and ABS contributions to the photoresponse. This establishes a new gap spectroscopy tool that is sensitive to nodes in the superconducting gap accessed by currents flowing in the plane of the material, and can detect gap nodes directly, or indirectly through Andreev bound states, through their influence on the in-plane electrodynamics in the superconducting state.

We thank D. J. Scalapino, I. Mazin, and V. Yakovenko for helpful discussions. The work at Maryland was supported by ONR Grants No. N000140811058 and No. 20101144225000, the US DOE DESC 0004950, the ONR AppEl Center, Task D10 (N000140911190), and CNAM. The work in Karlsruhe is supported by the

Deutsche Forschungsgemeinschaft (DFG) and the State of Baden-Württemberg through the DFG-CFN, and a NASU program on Nanostructures, Materials, and Technologies. S. M. A. acknowledges sabbatical support from the CFN at KIT.

[1] J. Bardeen, Phys. Rev. Lett. **1**, 399 (1958); R. H. Parmenter, RCA Rev. **23**, 323 (1962); J. Gittleman, B. Rosenblum, T. E. Seidel, and A. W. Wicklund, Phys. Rev. **137**, A527 (1965).
[2] S. K. Yip and J. A. Sauls, Phys. Rev. Lett. **69**, 2264 (1992).
[3] D. Xu, S. K. Yip, and J. A. Sauls, Phys. Rev. B **51**, 16233 (1995).
[4] T. Dahm and D. J. Scalapino, J. Appl. Phys. **81**, 2002 (1997).
[5] T. Dahm and D. J. Scalapino, Appl. Phys. Lett. **69**, 4248 (1996).
[6] T. Dahm and D. J. Scalapino, Phys. Rev. B **60**, 13125 (1999).
[7] M. R. Li, P. J. Hirschfeld, and P. Wolfle, Phys. Rev. Lett. **81**, 5640 (1998).
[8] J. Buan, B. P. Stojkovic, N. E. Israeloff, A. M. Goldman, C. C. Huang, O. T. Valls, J. Z. Liu, and R. Shelton, Phys. Rev. Lett. **72**, 2632 (1994).
[9] A. Bhattacharya, I. Zutic, O. T. Valls, A. M. Goldman, U. Welp, and B. Veal, Phys. Rev. Lett. **82**, 3132 (1999).
[10] A. Carrington, R. W. Giannetta, J. T. Kim, and J. Giapintzakis, Phys. Rev. B **59**, R14173 (1999).
[11] C. P. Bidinosti, W. N. Hardy, D. A. Bonn, and R. Liang, Phys. Rev. Lett. **83**, 3277 (1999).
[12] K. Halterman, O. T. Valls, and I. Zutic, Phys. Rev. B **63**, 180405 (2001).
[13] A. Maeda, Y. Iino, T. Hanaguri, N. Motohira, K. Kishio, and T. Fukase, Phys. Rev. Lett. **74**, 1202 (1995).
[14] G. Benz, S. Wünsch, T. A. Scherer, M. Neuhaus, and W. Jutzi, Physica (Amsterdam) **356C**, 122 (2001).
[15] D. E. Oates, S. H. Park, and G. Koren, Phys. Rev. Lett. **93**, 197001 (2004).
[16] K. T. Leong, J. C. Booth, and S. A. Schima, IEEE Trans. Appl. Supercond. **15**, 3608 (2005).
[17] I. Vekhter, P. J. Hirschfeld, J. P. Carbotte, and E. J. Nicol, Phys. Rev. B **59**, R9023 (1999).
[18] H. Aubin, K. Behnia, M. Ribault, R. Gagnon, and L. Taillefer, Phys. Rev. Lett. **78**, 2624 (1997).
[19] T. Park, M. B. Salamon, E. M. Choi, H. J. Kim, and S.-I. Lee, Phys. Rev. Lett. **90**, 177001 (2003).
[20] A measurement of the aNLME in the conventional superconductor Nb has been demonstrated by N. Groll, A. Gurevich, and I. Chiorescu, Phys. Rev. B **81**, R020504 (2010).
[21] I. Žutić and O. T. Valls, Phys. Rev. B **56**, 11279 (1997).
[22] C.-R. Hu, Phys. Rev. Lett. **72**, 1526 (1994).
[23] M. Fogelström, D. Rainer, and J. A. Sauls, Phys. Rev. Lett. **79**, 281 (1997).
[24] M. Aprili, E. Badica, and L. H. Greene, Phys. Rev. Lett. **83**, 4630 (1999).
[25] H. Walter, W. Prusseit, R. Semerad, H. Kinder, W. Assmann, H. Huber, H. Burkhardt, D. Rainer, and J. A. Sauls, Phys. Rev. Lett. **80**, 3598 (1998).
[26] A. Carrington, F. Manzano, R. Prozorov, R. W. Giannetta, N. Kameda, and T. Tamegai, Phys. Rev. Lett. **86**, 1074 (2001).
[27] Yu. Barash, M. S. Kalenkov, and J. Kurkijärvi, Phys. Rev. B **62**, 6665 (2000).
[28] A. Zare, T. Dahm, and N. Schopohl, Phys. Rev. Lett. **104**, 237001 (2010).
[29] C. Kurter, J. Abrahams, and S. M. Anlage, Appl. Phys. Lett. **96**, 253504 (2010).
[30] S. M. Anlage, J. Optics **13**, 024001 (2011).
[31] C. Kurter, A. P. Zhuravel, J. Abrahams, C. L. Bennett, A. V. Ustinov, and S. M. Anlage, IEEE Trans. Appl. Supercond. **21**, 709 (2011).
[32] C. Kurter, A. P. Zhuravel, A. V. Ustinov, and S. M. Anlage, Phys. Rev. B **84**, 104515 (2011).
[33] A. P. Zhuravel, C. Kurter, A. V. Ustinov, and S. M. Anlage, Phys. Rev. B **85**, 134535 (2012).
[34] See Supplemental Material at http://link.aps.org/supplemental/10.1103/PhysRevLett.110.087002 for the principle of operation of the laser scanning microscope, and discussion of the PR phase and dependence on laser intensity.
[35] D. W. Face, C. Wilker, J. J. Kingston, Z.-Y. Shen, F. M. Pellicone, R. J. Small, S. P. McKenna, S. Sun, and P. J. Martin, IEEE Trans. Appl. Supercond. **7**, 1283 (1997).
[36] http://www.theva.com/user/eesy.de/theva.biz/dwn/Datasheet_Coatings.pdf.
[37] A. P. Zhuravel, A. G. Sivakov, O. G. Turutanov, A. N. Omelyanchouk, S. M. Anlage, A. Lukashenko, A. V. Ustinov, and D. Abraimov, Low Temp. Phys. **32**, 592 (2006).
[38] A. P. Zhuravel, S. M. Anlage, S. K. Remillard, A. V. Lukashenko, and A. V. Ustinov, J. Appl. Phys. **108**, 033920 (2010).
[39] H. S. Newman and J. C. Culbertson, Microw. Opt. Technol. Lett. **6**, 725 (1993); J. C. Culbertson, H. S. Newman, and C. Wilker, J. Appl. Phys. **84**, 2768 (1998).
[40] A. P. Zhuravel, A. V. Ustinov, K. S. Harshavardhan, and S. M. Anlage, Appl. Phys. Lett. **81**, 4979 (2002).
[41] D. J. Scalapino (private communication).
[42] Y. M. Wang, W. Wan, R. Wang, F. H. Li, and G. C. Che, Philos. Mag. Lett. **88**, 481 (2008).
[43] This apparent rotation occurs over a narrow temperature range because of the two competing PR contributions with opposite signs and very different temperature dependencies.
[44] S. Streiffer, E. M. Zielinski, B. M. Lairson, and J. C. Bravman, Appl. Phys. Lett. **58**, 2171 (1991).
[45] G. Kästner, C. Schäfer, St. Senz, T. Kaiser, M. A. Hein, M. Lorenz, H. Hochmuth, and D. Hesse, Supercond. Sci. Technol. **12**, 366 (1999).
[46] K. An, T. Sakakibara, R. Settai, Y. Onuki, M. Hiragi, M. Ichioka, and K. Machida, Phys. Rev. Lett. **104**, 037002 (2010).
[47] B. Zeng, G. Mu, H. Q. Luo, T. Xiang, I. I. Mazin, H. Yang, L. Shan, C. Ren, P. C. Dai, and H.-H. Wen, Nat. Commun. **1**, 112 (2010).
[48] A. B. Vorontsov and I. Vekhter, Phys. Rev. B **75**, 224501 (2007).
[49] E. T. Swartz and R. O. Pohl, Rev. Mod. Phys. **61**, 605 (1989).